

# Original Research

## D4F alleviates the C/EBP homologous protein-mediated apoptosis in glycosylated high-density lipoprotein-treated macrophages by facilitating autophagy

Hua Tian<sup>1,2</sup> , Zhaoqiang Zhang<sup>3</sup>, Xiaoyan Han<sup>4</sup>, Tianqi Pan<sup>3</sup>, Geru Tao<sup>1</sup>, Peng Jiao<sup>1</sup>, Lei Zhai<sup>1</sup>, Libo Yang<sup>5</sup>, Xiaoxu Wang<sup>3</sup>, Yilin Yao<sup>3</sup>, Shucun Qin<sup>1</sup> and Shutong Yao<sup>1,3</sup>

<sup>1</sup>Key Laboratory of Atherosclerosis in Universities of Shandong and Institute of Atherosclerosis, Shandong First Medical University & Shandong Academy of Medical Sciences, Taian 271000, China; <sup>2</sup>College of Traditional Chinese Medicine, Shandong University of Traditional Chinese Medicine, Jinan 250355, China; <sup>3</sup>College of Basic Medical Sciences, Shandong First Medical University & Shandong Academy of Medical Sciences, Taian 271000, China; <sup>4</sup>College of Stomatology, Shandong First Medical University & Shandong Academy of Medical Sciences, Taian 271000, China; <sup>5</sup>Department of Endocrinology, Central Hospital of Taian, Taian 271000, China  
Corresponding authors: Hua Tian. Email: liutianfangyu@163.com; Shutong Yao. Email: yst228@126.com

### Impact statement

D4F, the mimetic peptide of apolipoprotein A-I, exerts antiatherogenic effects. Our study demonstrated that D4F inhibited gly-HDL-induced cell apoptosis by restraining the ERS-C/EBP homologous protein pathway. More importantly, D4F facilitates the gly-HDL-triggered activation of autophagy in macrophages. Furthermore, administering D4F to T2DM mice upregulated LC3-II and attenuated CHOP expression, cell apoptosis, and atherosclerotic lesions. These results suggested that D4F protects macrophages against gly-HDL-induced ER stress-CHOP-mediated apoptosis by promoting autophagy and increases the stability of atherosclerotic plaques. Therefore, D4F may be applied in the clinical pharmacological treatment of AS in T2DM.

### Abstract

The present study aimed to investigate the role of D4F, an apolipoprotein A-I mimetic peptide, in macrophage apoptosis induced by the glycosylated high-density lipoprotein (gly-HDL)-induced endoplasmic reticulum (ER) stress C/EBP homologous protein (CHOP) pathway, and unravel the regulatory role of autophagy in this process. Our results revealed that except for suppressing the accumulation of lipids within RAW264.7 macrophages caused by gly-HDL, D4F inhibited gly-HDL-induced decrease in the cell viability and increase in lactate dehydrogenase leakage and cell apoptosis, which were similar to 4-phenylbutyric acid (PBA, an ER stress inhibitor). Besides, similar to PBA, D4F inhibited gly-HDL-induced ER stress response activation evaluated through the decreased PERK and eIF2 $\alpha$  phosphorylation, together with reduced ATF6 nuclear translocation as well as the downregulation of GRP78 and CHOP. Interestingly, D4F facilitated gly-HDL-triggered activation of autophagy, measured as elevated levels of beclin-1, LC3-II, and ATG5 expressions in macrophages. Furthermore, the inhibition effect of D4F on gly-HDL-induced ER stress-CHOP-induced

apoptosis of macrophages was restrained after beclin-1 siRNA and 3-methyladenine (3-MA, an inhibitor of autophagy) treatments, while this effect was further reinforced after rapamycin (Rapa, an inducer of autophagy) treatment. Furthermore, administering D4F or Rapa to T2DM mice upregulated LC3-II and attenuated CHOP expression, cell apoptosis, and atherosclerotic lesions. However, the opposite results were obtained when 3-MA was administered to these mice. These results support that D4F effectively protects macrophages against gly-HDL-induced ER stress-CHOP-mediated apoptosis by promoting autophagy.

**Keywords:** D4F, autophagy, apoptosis, C/EBP homologous protein, macrophages, glycosylated high-density lipoprotein

*Experimental Biology and Medicine* 2021; 246: 2595–2609. DOI: 10.1177/15353702211045323

### Introduction

Atherosclerosis (AS) is the pathological basis of the peripheral arterial disorder, stroke, and coronary heart disease (CHD), and also the main reason underlying the incidence and mortality of cases with dyslipidemia and diabetes

mellitus (DM).<sup>1,2</sup> Hyperglycemia may exacerbate atherosclerotic progression by inducing oxidative stress, promoting inflammation,<sup>3</sup> and heightening the susceptibility to AS in vascular smooth muscle cells (VSMCs).<sup>4</sup> In this pathophysiological process, advanced glycation end-products

(AGEs) possibly play vital roles by inhibiting the reverse cholesterol transport from macrophages, promoting inflammation, and forming oxidized low-density lipoprotein (ox-LDL).<sup>5,6</sup> High-density lipoprotein (HDL) has been confirmed to exhibit antiatherosclerotic properties including anti-oxidation, anti-inflammation, and reverse cholesterol transport, while glycation of HDL damages the antiatherogenic functions of HDL.<sup>7,8</sup> Previous studies, including the ones by our research group, have demonstrated that glycated HDL (gly-HDL) possibly induces apoptosis of macrophage and endothelial cells, which has been recognized as a crucial step in the progression of atherosclerosis and formation of unstable plaque.<sup>9,10</sup> Endoplasmic reticulum (ER) stress-mediated apoptotic pathway is recognized as the key mechanism of cell apoptosis. In ER stress, C/EBP homologous protein (CHOP) is a vital proapoptotic molecule, which exerts an important effect on macrophage apoptosis as well as on DM and AS development, especially in the instability of atherosclerotic plaques.<sup>11,12</sup> In recent research, we demonstrated that gly-HDL and ox-HDL promote the apoptosis of macrophages via the CHOP pathway.<sup>10,13</sup> Therefore, inhibiting the apoptosis of macrophages via the ER stress-CHOP pathway may serve as a potential treatment approach for AS.

D4F, the apolipoprotein-AI mimetic peptide (a major antiatherogenic functional component of HDL) that contains 18 amino acids, contains the class A amphipathic helix that allows for binding to lipids similar to apo AI.<sup>14,15</sup> An increasing number of studies suggest that D4F suppresses AS, including the improvement of reverse cholesterol transport,<sup>16,17</sup> reduction in the chemotactic activity of ox-LDL-mediated monocytes, and enhancement of the HDL anti-inflammation.<sup>18</sup> Moreover, D4F decreases the formation of AS lesions in mice, irrespective of the cholesterol content in the plasma (high or low). In addition, D4F may eliminate the oxidized lipids out of the lipoproteins.<sup>19</sup> As reported in our previous study, D4F decreases the human umbilical vein endothelial cell cytotoxicity mediated by ox-LDL by promoting pigment epithelium-derived factor and inhibits the apoptosis of macrophages by inactivating the NF- $\kappa$ B-Fas/FasL death receptor pathway.<sup>20,21</sup> Nonetheless, the mechanism by which D4F affects CHOP-mediated apoptosis in gly-HDL-treated macrophages remains unclear so far.

Autophagy is a kind of cell decomposition and recycling process, which functions for maintaining energy balance and quality control by obliterating the misfolded proteins and dysfunctional subcellular organelles in lysosomes.<sup>22</sup> Accumulating evidence has demonstrated that autophagy promotes cell survival under various stimuli, including ER stress, metabolic stress, and oxidative stress,<sup>23–25</sup> besides, it protects against advanced AS.<sup>26,27</sup> Data from our recent studies revealed that autophagy response inhibits gly-HDL-induced macrophage apoptosis through the partial alleviation of the ER stress-CHOP pathway.<sup>10</sup> The present study focused on investigating the influence of D4F on the apoptosis mediated by the ER stress-CHOP pathway and the autophagy response in this apoptosis process in gly-HDL-treated macrophages and type 2 diabetes mellitus (T2DM) apoE<sup>-/-</sup> mice.

## Materials and methods

### Reagents

Oil red O, 3-methyladenine (3-MA), rapamycin (Rapa), 4-phenylbutyric acid (PBA), and streptozotocin (STZ) were obtained from Sigma-Aldrich (St Louis, MO, USA). Carboxymethyl lysine (CML) ELISA kit was provided by BlueGene Biotech (Shanghai, China), and the Annexin V-FITC apoptosis detection kit was provided by KeyGEN Biotech (Nanjing, China). Lactate dehydrogenase (LDH) and TUNEL (TMR red, In Situ Cell Death Detection kit) detection kits were obtained from Solarbio (Beijing, China) and Roche (Mannheim, Germany), respectively. The Cell Counting Kit-8 reagent (CCK-8) was obtained from Beyotime (Dojindo Laboratories, Kumamoto, Japan). The monocyte plus macrophage (MOMA-2, ab33451) rat antibody, C/EBP homologous protein (CHOP, ab63392, ab11419), glucose-regulated protein 78 (GRP78, ab21685), and the activating transcription factor 6 (ATF6, ab37149) rabbit antibodies were purchased from Abcam (Cambridge, MA, USA). The phospho-eukaryotic translation initiation factor 2 $\alpha$  (p-eIF2 $\alpha$ , sc293100) and the phospho-double-stranded RNA-activated protein kinase-like ER kinase (p-PERK, sc32577) rabbit antibodies were purchased from Santa Cruz Biotechnology (Santa Cruz, CA, USA). In addition, the microtubule-associated protein 1 light chain 3 (LC3, L7543), beclin-1 (PRS3613), and autophagy-related gene 5 (ATG5, A0731) rabbit antibodies were obtained from Sigma-Aldrich (St Louis, MO, USA). The Alexa Fluor 594-labeled donkey anti-rat (A32758) and Alexa Fluor 488-labeled donkey anti-rabbit (A21206) antibodies were obtained from Molecular Probes (Eugene, OR, USA). D-4F (Ac-DWFKAFYDKVAEKFKAEAF-NH<sub>2</sub>) and scrambled D4F (Ac-DWFAKDYFKKAFVEEFAK-NH<sub>2</sub>) were synthesized from Scilight Biotechnology (Beijing, China).

### Preparation of gly-HDL

Gly-HDL was prepared as described in a previous study.<sup>28,29</sup> In brief, the plasma native HDL (density = 1.063–1.210 g/mL) was extracted from normolipidemic donors using density-gradient ultracentrifugation, followed by seven days of incubation in the dark with glucose (50 mmol/L) in PBS solution containing 2 mmol/L ethylene diamine tetraacetic acid (EDTA) under nitrogen, sterile conditions, and 37°C. The glycation modification reaction was terminated through thorough dialysis in PBS (pH = 7.4) containing 1 mmol/L EDTA for removing the free glucose. The glycation extent in HDL was assessed by detecting the CML level via ELISA. The CML level in gly-HDL was 202.4  $\pm$  58.8 pg/mg protein. The endotoxin level in the prepared HDL was detected using the Limulus Amoebocyte Lysate kit (Bio Whittaker, Walkersville, MD); however, no endotoxin was detected in the HDL prepared in the present work (<50 pg/mg protein).

### Cell culture and siRNA transfection

The RAW264.7 cells were procured from the American Type Culture Collection (ATCC), Chinese Academy of Sciences, and cultured in DMEM medium containing 10% (v/v) fetal bovine serum (FBS) under 5% CO<sub>2</sub> atmosphere and at 37°C. Later, the original medium was replaced with 1% FBS-containing DMEM prior to applying the different treatments.

Lipofectamine 2000 (Invitrogen, Carlsbad, CA, USA) was used for transfecting the cells with specific small interfering RNA (siRNA) oligomers targeting beclin-1 (200 pmol), which was achieved by incubation for 48 h and using specific protocols; control siRNA oligomers were used as the negative reference. Afterward, gly-HDL (100 mg/L) was employed to treat the cells for 24 h. Beclin-1 siRNA (5'-GUAUAUUAACCACAUGUdTdT-3') and Control siRNA (5'-UUCUCCGAACGUGUCACGUTT-3') (SASI\_Mm01\_00048151) were provided by Sigma-Aldrich. Silencing of the target gene was verified through Western blotting assay.

### Animals and the experimental design

The C57BL/6 and apoE<sup>-/-</sup> male mice (6-week-old) were procured from Huafukang Biotechnology (Beijing, China). The Ethical Committee for the Use of Laboratory Animals, Shandong First Medical University, approved the animal experiment procedures to be used in the present study. All procedures were performed by following the relevant guidelines.

The T2DM apoE<sup>-/-</sup> mice models were established as described in a previous study.<sup>30</sup> In brief, after one week of acclimatization, the apoE<sup>-/-</sup> mice were raised on a high-fat diet containing 20% sugar, 20% fat, and 1.25% cholesterol for eight weeks. Thereafter, intraperitoneal glucose tolerance test was conducted to identify the insulin-resistant mice with blood glucose levels much higher than blood glucose levels in normal chow diet-fed apoE<sup>-/-</sup> mice at 15, 30, 60 and 90 min. Subsequently, 75 mg/kg streptozotocin (STZ) was administered to the insulin-resistant mice intraperitoneally to induce partial insulin deficiency. After two weeks, the animals exhibiting random fasting blood glucose (FBG) > 11.1 mmol/L in one or more of the three independent tests were considered T2DM mice; these mice were then randomly divided into four groups based on different treatments: model group was intraperitoneally injected with vehicle (Model group, n = 8); D4F group (D4F, 1 mg/kg/d, n = 8); 3-MA group (3-MA, 50 mg/kg/d, n = 8); Rapa group (Rapa, 6 mg/kg/d, n = 8) once a day for additional 8 weeks. A regular normal chow diet was fed to 8 male C57BL/6 mice in the normal control group, followed by an intraperitoneal injection of an equal volume of saline containing 0.1% Tween-80. At the completion of the experiment, the animals were sacrificed for the collection of hearts with the proximal aorta and aortic archs. The hearts were embedded in the optimal cutting temperature (OCT) compound and frozen at -80°C for oil red O staining, TUNEL, and immunofluorescence analysis. The aortic archs were stored at -80°C for the Western blotting.

### Lipid determination

In order to observe the lipid droplets within macrophages, the RAW264.7 cells were seeded onto the cover glass in the six-well tissue culture plates, followed by washing with PBS and a 20-min fixation in 4% paraformaldehyde. Subsequently, the cells were washed with PBS and then subjected to 30 min of oil red (0.5% in isopropanol) staining at room temperature; after washing with PBS, the cells were then re-stained with hematoxylin for 2 min. Next, the stained cells were observed and photographed under Olympus BX53 microscope (Olympus, Tokyo, Japan), and the Image-Pro Plus image analysis software (Media Cybernetics, LP, USA) was used for determining the lipid droplet content. Results were presented as the means of the integrated optical density (IOD) for each cell.

Next, Nile red staining was performed to determine the lipid content in the cells. Cells were rinsed with PBS and subjected to Nile red treatment (1 µg/mL) under ambient temperature for 20 min. Finally, at least 10,000 stained cells each group were rinsed and resuspended with PBS, and then detected using the FAC Scan flow cytometer (Becton Dickinson, San Jose, CA, USA) at the emission and excitation wavelengths at 590 and 568 nm, respectively. Results were presented as the average fluorescence intensity.

In order to analyze the AS lesions, brilliant green and oil red O were used for staining the 8-µm aortic root cryosections. The AS lesions were observed under a microscope (Olympus BX53, Tokyo, Japan), and five sections were examined from each mouse to calculate the overall average plaque area (µm<sup>2</sup>) using Image-Pro Plus software.

### CCK-8 and LDH assays

RAW264.7 cells (5 × 10<sup>3</sup>/well) were seeded into 96-well plates for 24 h. Then, the cells were treated with 10 µL CCK-8 solution for 2 h. Next, optical densities (ODs) were measured at 450 nm in a microplate reader (Spectramax i3x, USA). The ratio of the CCK-8 count in the treated cells to that in the untreated controls was calculated as the cell viability (100%).

In order to better evaluate cell injury, a specific detection kit was employed for measuring the cellular LDH release into the medium using specific protocols.

### Apoptosis measured through flow cytometry

Annexin V-FITC/PI double-staining detection kit was used for measuring the apoptosis of Raw264.7 cells. Briefly, the exposed cells were rinsed with PBS and incubated in the dark with 500 µL binding buffer containing 5 µL Annexin V-FITC/propidium iodide (PI) for 15 min at room temperature. Thereafter, all stained cells were examined under the FAC scan flow cytometer equipped with Cell-Quest software (Becton Dickinson, San Jose, CA, USA).

### TUNEL analysis

The treated RAW264.7 cells on glass cover slips in six-well plates or mouse aortic root cryosections were washed with PBS. Next, the cells and aortic roots were fixed in 4% paraformaldehyde for 20 min. After washing with PBS, 0.1%

Triton X-100 was added for 2 min for cell permeabilization. Finally, the TUNEL reaction mixture was added to allow for reaction with cells and aortic roots on ice in the dark for 1 h, followed by 4',6-diamidino-2-phenylindole (DAPI) treatment for 5 min at room temperature. Morphology of cells and aortic roots were observed under a fluorescence microscope (Olympus BX53, Tokyo, Japan). TUNEL-positive cell number among the overall cell count or the AS lesion area was considered the cell apoptosis ratio. At least five field of views each section of each group were obtained and analyzed.

### Immunofluorescence

RAW264.7 cells were seeded onto the circular coverslips in the six-well plates. After washing with PBS, cells were fixed in 4% paraformaldehyde for 20 min. After another rinse with PBS, cells were permeabilized using 0.1% Triton-X-100 at ambient temperature, blocked using normal donkey serum, and subsequently incubated overnight with anti-ATF6 or anti-LC3 antibody at 1:200 dilution under 4°C. Following 30 min of incubation with Alexa Fluor 488-labeled secondary antibody at room temperature, DAPI was used for counterstaining the cells. The stained cells were visualized under a confocal microscope (Bio-Rad Radiance 2100). ATF6 immunofluorescence and LC3-labeled autophagosomal puncta accumulation were analyzed digitally using Image-Pro Plus software. At least five field of views each section of each group were obtained and analyzed.

The normal donkey serum was used for blocking the serial aortic root frozen sections (8 µm), and then the anti-MOMA-2, anti-LC3, and anti-CHOP primary antibodies at 1:200 dilution were incubated overnight with the cells under 4°C. Thereafter, the frozen sections were exposed to Alexa Fluor 488-labeled donkey anti-rabbit and Alexa Fluor 594-labeled donkey anti-rat secondary antibody treatments for 30 min, followed by counterstaining with DAPI. A fluorescence microscope (Olympus BX53, Tokyo, Japan) was utilized to observe and digitally analyze the captured images. Image-Pro Plus software was utilized to measure the average fluorescence intensity in the AS plaque. At least five field of views each section of each group were obtained and analyzed.

### Western blot analysis

PMSF-containing RIPA lysis buffer and nuclear extraction kits were used for isolating total proteins from the aortic tissues and the total and nuclear proteins from treated RAW264.7 cells, respectively. Afterward, the cells were subjected to 30 min of centrifugation at 12,000 × g and 4°C; 10% SDS-PAGE was used to separate equal amounts of proteins (40 µg), followed by transfer of the protein bands onto the PVDF membranes. Milk was used to block each membrane, followed by an overnight incubation with primary antibodies under 4°C, including anti-p-PERK (1:500), anti-p-eIF2α (1:500), anti-GRP78 (1:200), anti-CHOP (1:200), anti-beclin-1 (1:200), anti-ATG5 (1:200), and anti-LC3 (1:500). Then, incubation with goat anti-rabbit IgG secondary antibody conjugated with HRP (1:1,500) was performed

for 2 h at ambient temperature. Next, the enhanced chemiluminescence kit was utilized to analyze the proteins; band intensity was quantified using Image-Pro Plus software, followed by normalization relative to the reference (histone or β-actin).

### Statistical analysis

Data are presented as mean ± standard deviation. One-way ANOVA was performed for statistical analysis using SPSS 16.0, in which two groups were compared using the Student's *t*-test, while the Student–Newmann–Keuls test was employed in the case of several groups. The *p*-value of <0.05 represented a statistically significant difference.

## Results

### D4F mitigated gly-HDL-induced lipid accumulation within RAW264.7 cells

Our previous studies showed that gly-HDL and ox-LDL induced lipid accumulation in macrophage cells, while D4F inhibited the ox-LDL-induced accumulation of intracellular lipids.<sup>10,31</sup> The results of the present study confirmed that D4F treatment (12.5, 25, 50 mg/L), but not sD4F (an inactive scrambled peptide control), significantly reduced the gly-HDL-induced accumulation of intracellular lipids in a dose-dependent manner (Figure 1).

### D4F protected against gly-HDL-mediated apoptosis and cytotoxicity of RAW264.7 cells

In order to investigate the cytoprotective role of D4F in macrophages, we detected the LDH activity and cell viability using LDH assay kits and CCK-8 assay, respectively. The results showed that gly-HDL treatment significantly decreased cell viability and increased LDH release, which inhibited by D4F pretreatment in a dose-dependent manner (Figure 2(a) and (b)). PBA (an ER stress inhibitor), but not sD4F, also blocked the reduced cell viability and increased LDH leakage induced by gly-HDL.

Next, Annexin V-FITC/PI double-staining and TUNEL staining were performed to evaluate the anti-apoptotic effect of D4F. As presented in Figure 3(a) and (b), the proportion of apoptotic cells remarkably elevated at 24 h after the gly-HDL treatment, which declined strongly after D4F treatment in a dose-dependent manner and PBA treatment. The above findings indicated the potential role of D4F in the inhibition of gly-HDL-mediated macrophage injury and apoptosis through the inhibition of the ER stress pathway.

### D4F mitigated gly-HDL-induced ER stress response in RAW264.7 cells

We have demonstrated that gly-HDL induced apoptosis in RAW264.7 cells by activating the ER stress pathway. The present study also assessed the alterations occurring in CHOP and its two important upstream molecules, PERK and ATF6 *in vitro*, to illuminate the cytoprotective mechanism of D4F in the macrophages induced with gly-HDL treatment. Figure 3 illustrates that gly-HDL activated the

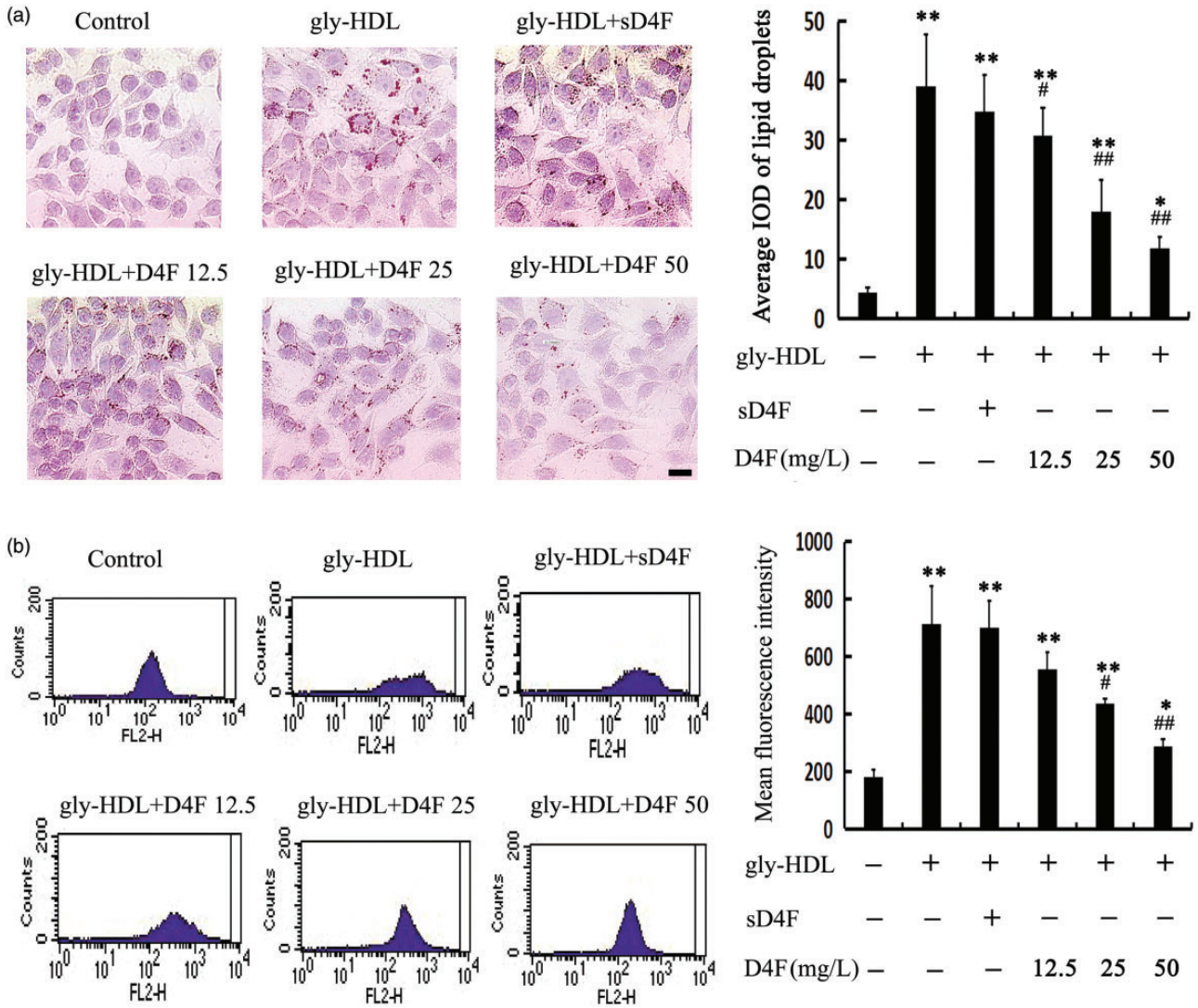


**Figure 1.** D4F reduces gly-HDL-induced accumulation of lipids in RAW264.7 cells. RAW264.7 cells were subjected to treatment with or without D4F (12.5, 25, 50 mg/L) or 50 mg/L of sD4F (inactive control peptide scrambled D4F) initially for 1 h and later for 24 h using 100 mg/L gly-HDL. Thereafter, the intracellular lipid contents were determined using oil red O staining (a) and Nile red staining (b), separately. Typical images for lipid droplet staining. Scale bar: 20  $\mu$ m;  $n = 5$ . Mean  $\pm$ SD. \* $P < 0.05$ , \*\* $P < 0.01$  vs. control group. # $P < 0.05$ , ## $P < 0.01$  vs. gly-HDL group. (A color version of this figure is available in the online journal.)

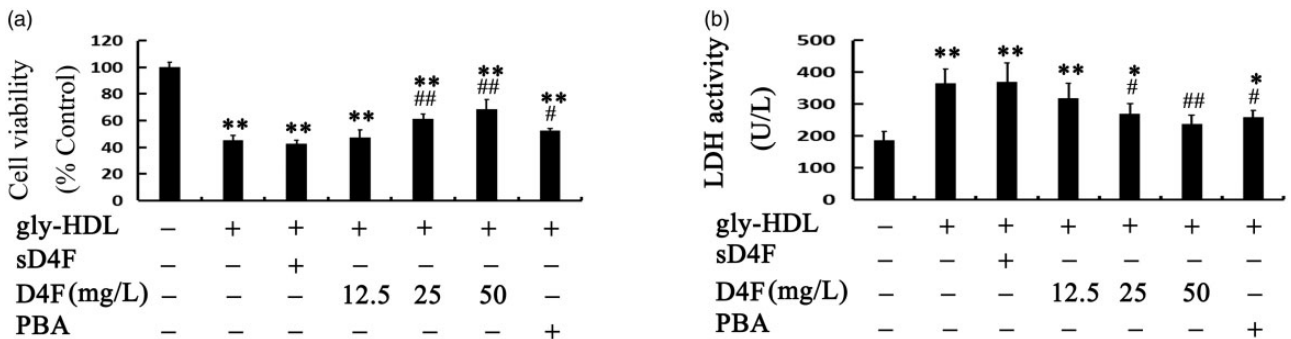


**Figure 2.** Role of D4F in gly-HDL-induced cytotoxicity of RAW264.7 cells. RAW264.7 cells were subjected to treatment with PBA (5 mmol/L), sD4F (50 mg/L), or D4F (12.5, 25, 50 mg/L) initially for 1 h and later for 24 h using gly-HDL (100 mg/L). (a and b) The CCK8 assay was conducted and LDH kits were used to measure the cell viability and LDH activity, respectively.  $n = 5$ , Mean  $\pm$ SD. \* $P < 0.05$ , \*\* $P < 0.01$  vs. control group. # $P < 0.05$ , ## $P < 0.01$  vs. gly-HDL group.

ER stress-CHOP pathway, as evidenced by ATF6 nuclear translocation (Figure 4(a) and (b)), PERK and eIF2 $\alpha$  phosphorylation, and enhanced CHOP and GRP 78 protein expression (Figure 4(c)). Nonetheless, the D4F or PBA

treatment, and not sD4F, dramatically suppressed the gly-HDL-induced ER stress response. These results suggested that D4F could inhibit the gly-HDL-induced macrophage ER stress-CHOP pathway.

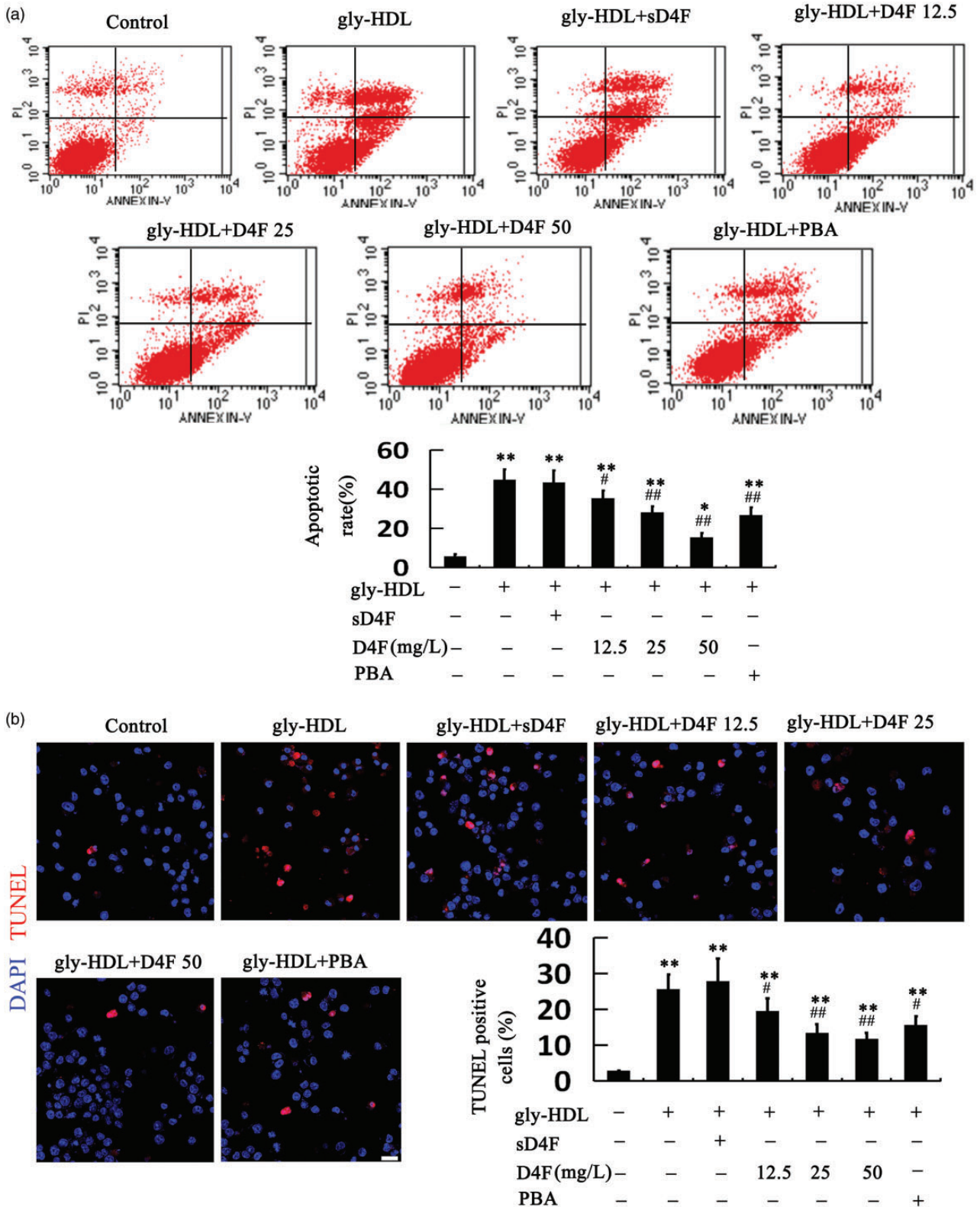


**Figure 3.** Role of D4F in gly-HDL-induced apoptosis of RAW264.7 cells. RAW264.7 cells were subjected to treatment with PBA (5 mmol/L), sD4F (50 mg/L), or D4F (12.5, 25, 50 mg/L) initially for 1 h and later for 24 h using gly-HDL (100 mg/L). (a) Cells were stained with Annexin-V-FITC/PI. Later, cell apoptosis was detected using flow cytometry. The overall apoptotic cell number (at both early and late stages) is presented on the right side of the panel (Annexin V in the absence or presence of PI). (b) Representative fluorescence micrographs depict TUNEL staining positive cells (red) and DAPI-stained nuclei (blue), while the graph presents the TUNEL-positive cell proportion corresponding to the overall cell number. Scale bar: 20  $\mu$ m; n = 5. Mean  $\pm$ SD. \* $P$  < 0.05, \*\* $P$  < 0.01 vs. control group. # $P$  < 0.05, ## $P$  < 0.01 vs. gly-HDL group. (A color version of this figure is available in the online journal.)

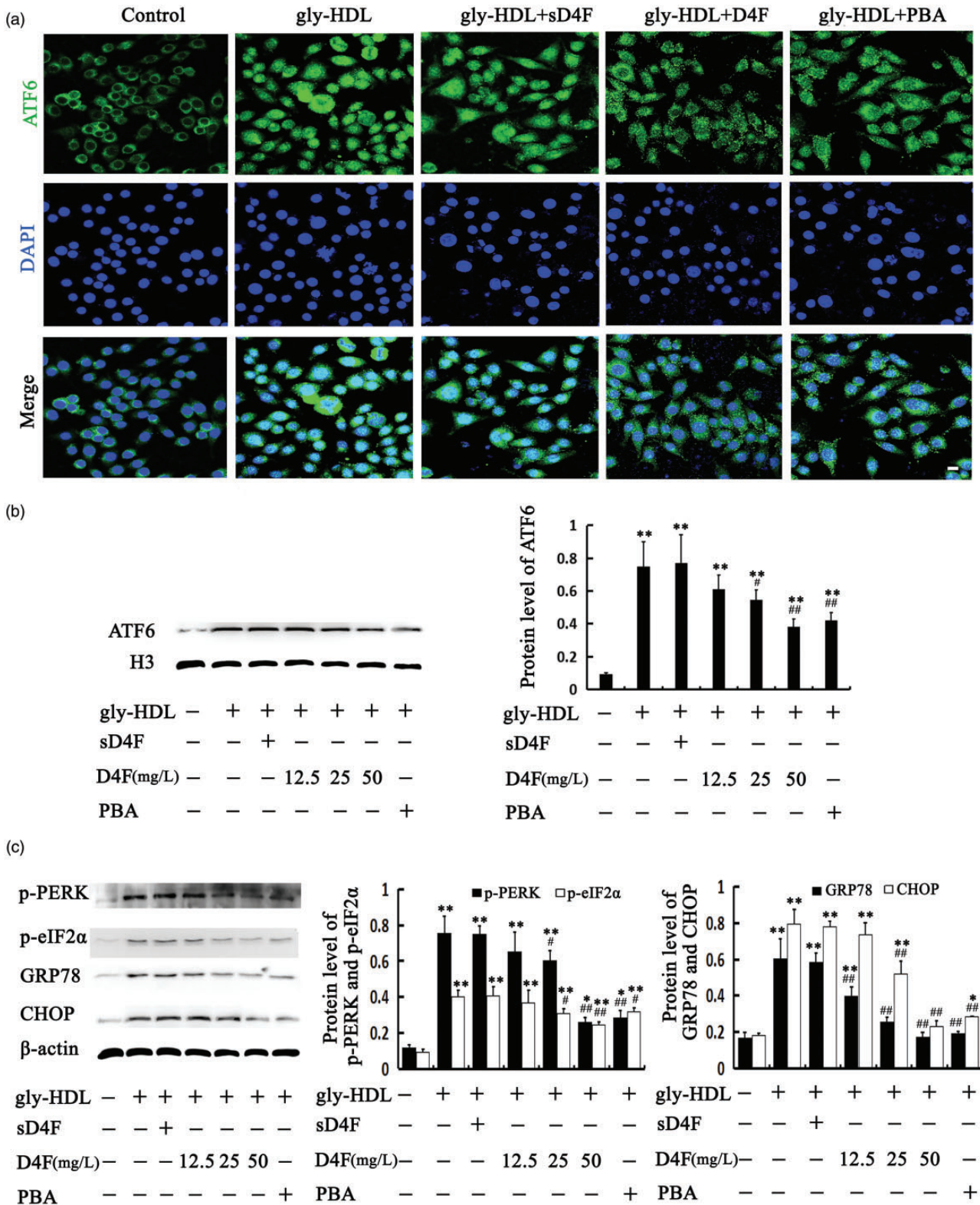


**Figure 4.** D4F inhibits gly-HDL-mediated ER stress response in RAW264.7 cells. RAW264.7 cells were subjected to treatment with PBA (5 mmol/L), sD4F (50 mg/L), or D4F (50 mg/L) initially for 1 h and later for 24 h using 100 mg/L gly-HDL. (a) Representative fluorescence confocal micrographs depicting ATF6 visualized through DAPI-stained nuclei (blue) and Alexa Fluor 488 (green). Scale bar: 20 μm; n = 5. (b and c) Cell treatments were identical to those depicted in Figure 2. ATF6, p-PERK, p-eIF2α, GRP78, and CHOP protein expressions were measured using Western blotting analysis. n = 4. Data are mean ± SD. \*P < 0.05, \*\*P < 0.01 vs. control group. #P < 0.05, ##P < 0.01 vs. gly-HDL group. (A color version of this figure is available in the online journal.)

### D4F facilitates gly-HDL-triggered RAW264.7 cell autophagy

According to our previous results, gly-HDL induced autophagy in RAW264.7 cells, which was evidenced by the elevated levels of autophagy markers, including ATG5, LC3-II, and beclin-1.<sup>10</sup> However, the level of autophagy triggered by gly-HDL was not sufficient to prevent gly-HDL-induced ER and stress-CHOP-induced RAW264.7 cell apoptosis. Since D4F suppressed gly-HDL-induced RAW264.7 cell apoptosis (Figure 3), it was hypothesized that D4F might facilitate gly-HDL-triggered autophagy to protect against macrophage apoptosis. In order to confirm this hypothesis, the role of D4F in autophagy response was assessed in the present study using immunofluorescence staining and Western blotting analysis. As expected, the green signal from LC3 puncta and the levels of autophagy-associated proteins, including beclin-1, ATG5, and LC3-II significantly increased in the gly-HDL-treated group relative to the control and D4F-treatment without gly-HDL. Moreover, preincubation of the cells with D4F, but not sD4F, further increased the green signal from LC3 puncta and the expression of the autophagy marker proteins compared to those in the gly-HDL-exposed cells in a dose-dependent manner (Figure 5(a) and (b)). These results revealed that D4F might further enhance the gly-HDL-induced autophagy in macrophages.

### D4F-facilitated autophagy inhibits CHOP-mediated apoptosis in gly-HDL-treated RAW264.7 cells

It is reported that the upregulation of macrophage autophagy attenuates cell death and AS.<sup>26,32,33</sup> In order to confirm the autophagic effect on the protective mechanism of D4F in ER stress-CHOP pathway-mediated apoptosis of macrophages treated by gly-HDL, this study used 3-methyladenine (3-MA, an autophagy inhibitor) and rapamycin (Rapa, an autophagy inducer) for inhibiting and inducing autophagy, respectively. As shown in Figure 6(a) to (c), the inhibitory effects of D4F on apoptosis, PERK phosphorylation, CHOP upregulation, and ATF6 nuclear translocation were further promoted by Rapa, while weakened by 3-MA in gly-HDL-treated RAW264.7 cells.

In order to further confirm the contribution of autophagy to the inhibition effect of D4F on gly-HDL-treated RAW264.7 cell apoptosis mediated by CHOP, beclin-1 siRNA was transfected into the cells prior to the gly-HDL treatment with or without D4F. Figure 7(a) and (b) suggested that beclin-1 siRNA pretreatment aggravated the cell apoptosis and CHOP expression induced by gly-HDL while eliminating the D4F influence on the above effects. These findings revealed that D4F suppressed ER stress-CHOP-apoptosis by enhancing gly-HDL-triggered autophagy in macrophages.

### Effects of D4F, 3-MA, and Rapa on atherosclerotic lesions and the expressions of LC3 and CHOP in type 2 diabetic apoE<sup>-/-</sup> mice

According to Figure 8(a) and (b), eight weeks of rapamycin or D4F treatment dramatically decreased cell apoptosis and

the area of atherosclerotic plaque in the aortic roots in T2DM apoE<sup>-/-</sup> mice compared to the vehicle-treated model mice. In contrast, the 3-MA treatment enhanced cell apoptosis as well as the plaque area. Furthermore, D4F and rapamycin evidently increased LC3-II expression and decreased CHOP expression in the aortic roots with abundant macrophages and aortic arches relative to the model group. However, converse data were obtained in the 3-MA treatment group (Figure 8(c) and (d)). These results indicated that similar to rapamycin, D4F might also inhibit CHOP upregulation and cell apoptosis in the atherosclerotic plaques in T2DM apoE<sup>-/-</sup> mice by promoting autophagy.

## Discussion

Hyperglycemia and dyslipidemia are strongly associated with the pathogenesis of atherosclerosis at all stages of the atherogenic process, and gly-HDL plays a crucial role in this process by activating the macrophage apoptosis pathway mediated by ER stress-CHOP.<sup>10</sup> As a consequence, inhibiting macrophage apoptosis mediated by ER stress-CHOP pathway is an effective treatment approach for combating atherosclerosis in patients with DM. The findings of the present work suggest that D4F decreased macrophage apoptosis mediated by the ER stress-CHOP pathway by facilitating autophagy, which was verified by the subsequent findings of the study. First, D4F reduced lipid accumulation in the macrophages along with injury and apoptosis induced by gly-HDL; these findings were consistent with the protective effect of PBA (an inhibitor of ER stress). Second, similar to PBA, D4F inhibited the ER stress-CHOP pathway by suppressing the activation of PERK and ATF6 together with CHOP upregulation induced by gly-HDL. Third, D4F facilitated gly-HDL-triggered autophagy; in addition, the inhibition effect of D4F on macrophage apoptosis mediated by ER stress-CHOP was weakened after beclin-1 siRNA and 3-MA (autophagy inhibitors) treatments, while it was further enhanced by Rapa (an autophagy inducer). Fourth, the administration of D4F to T2DM apoE<sup>-/-</sup> mice reduced the atherosclerotic plaque area and cell apoptosis, increased LC3-II expression, and decreased CHOP expression in macrophage-dense atherosclerotic lesions; these effects were similar to the protective effect of Rapa.

ApoA-I, as a major apolipoprotein of HDL, has been proven to protect against atherosclerosis by elevating the endothelial nitric oxide generation, enhancing reverse cholesterol transport, and suppressing LDL oxidation.<sup>14,15</sup> However, there are many limitations to the production and administration of ApoA-I containing 243 amino acids. ApoA-I mimetic peptides, which are synthetic peptide analogs containing 18 amino acids and possessing class A amphipathic helices secondary structural motif resembling apoA-I, have been designed and studied extensively.<sup>34</sup> D4F, an apoA-I mimetic peptide containing 4 phenylalanine (F) residues, is synthesized using D-amino acids and has been proven to attenuate atherosclerosis by increasing paraoxonase activity in HDL, improving reverse cholesterol transport, and promoting endothelial

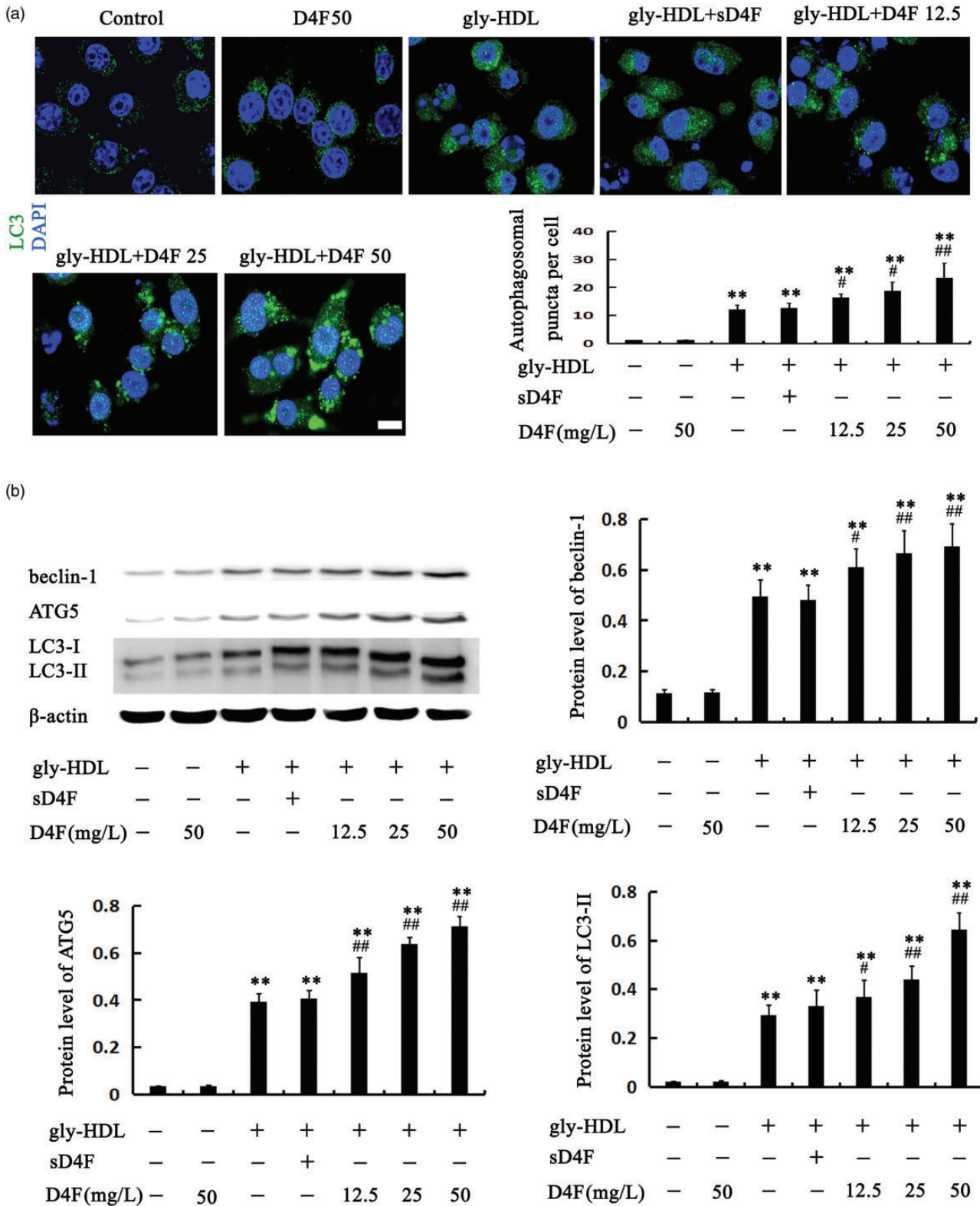


**Figure 5.** D4F promotes gly-HDL-triggered autophagy of RAW264.7 cells. RAW264.7 cells were subjected to treatment with sD4F (50 mg/L) or D4F (12.5, 25, 50 mg/L) initially for 1 h and later for 24 h using gly-HDL (100 mg/L). (a) Representative fluorescence confocal micrographs depicting DAPI-stained nuclei (blue) and Alexa Fluor 488-labeled LC3 (green). Autophagosomal puncta per cell were quantified. Scale bar: 20  $\mu$ m;  $n = 5$ . (b) Western blotting assay for assessing the beclin-1, ATG5, and LC3-II protein levels.  $n = 4$ . Mean  $\pm$ SD. \* $P < 0.05$ , \*\* $P < 0.01$  vs. control group. # $P < 0.05$ , ## $P < 0.01$  vs. gly-HDL group. (A color version of this figure is available in the online journal.)

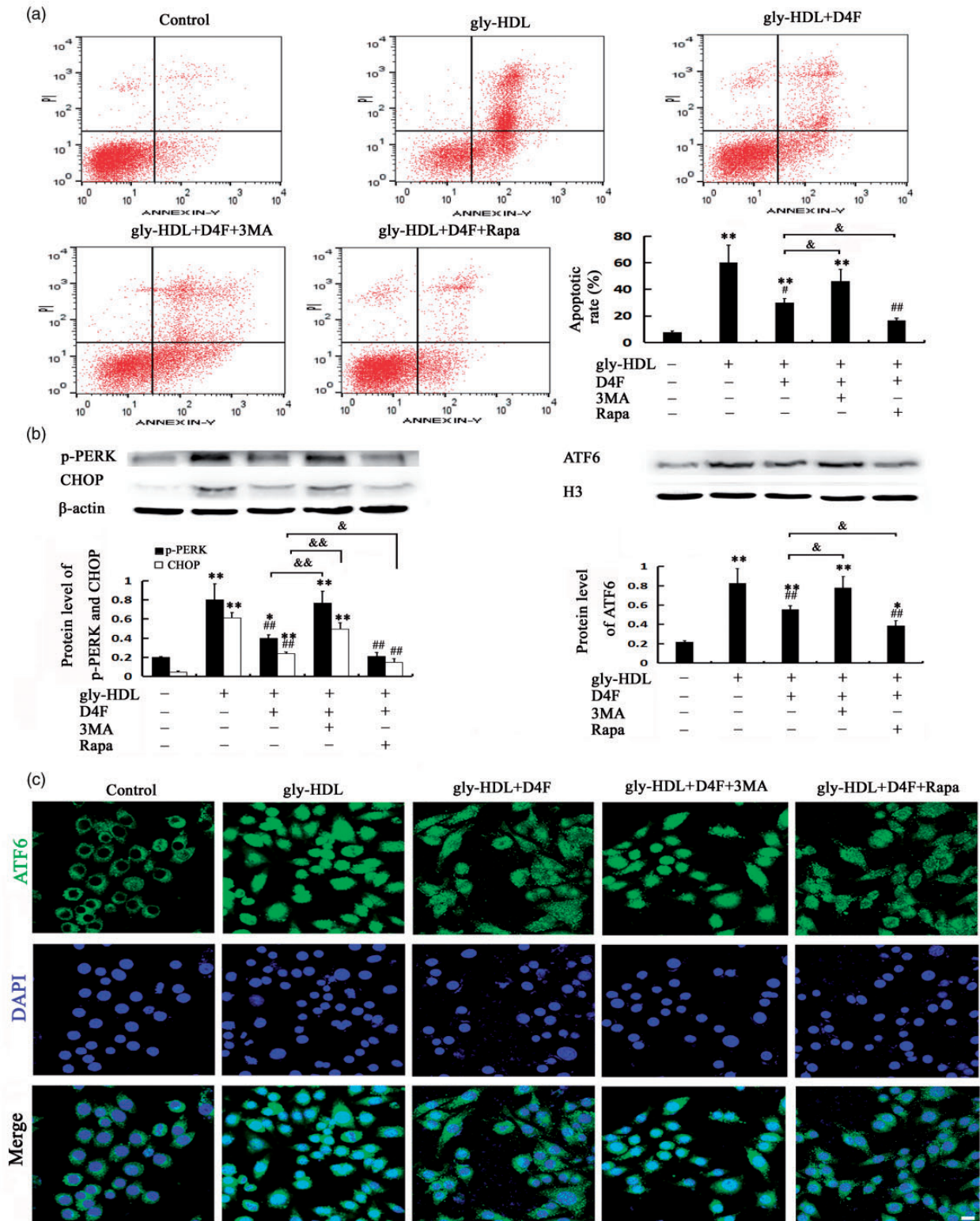


**Figure 6.** Autophagy facilitated by D4F inhibits CHOP-mediated apoptosis of RAW264.7 cells treated with gly-HDL. RAW264.7 cells were subjected to treatment with D4F (50 mg/L), rapamycin (Rapa, 1  $\mu$ mol/L) or 3-methyladenine (3-MA, 3 mmol/L) initially for 1 h and later for 24 h of treatment with gly-HDL (100 mg/L). (a) Cell apoptosis determined through flow cytometric analysis.  $n = 5$ . (b) Western blotting analysis to assess p-PERK, CHOP, and ATF6.  $n = 4$ . (c) Representative fluorescence confocal micrographs depicting DAPI-stained nuclei DAPI (blue) and Alexa Fluor 488-labeled ATF6 (green). Scale bar: 20  $\mu$ m;  $n = 5$ . Mean  $\pm$ SD. \* $P < 0.05$ , \*\* $P < 0.01$  vs. Control group; # $P < 0.05$ , ## $P < 0.01$  vs. gly-HDL group; & $P < 0.05$ , && $P < 0.01$ . (A color version of this figure is available in the online journal.)

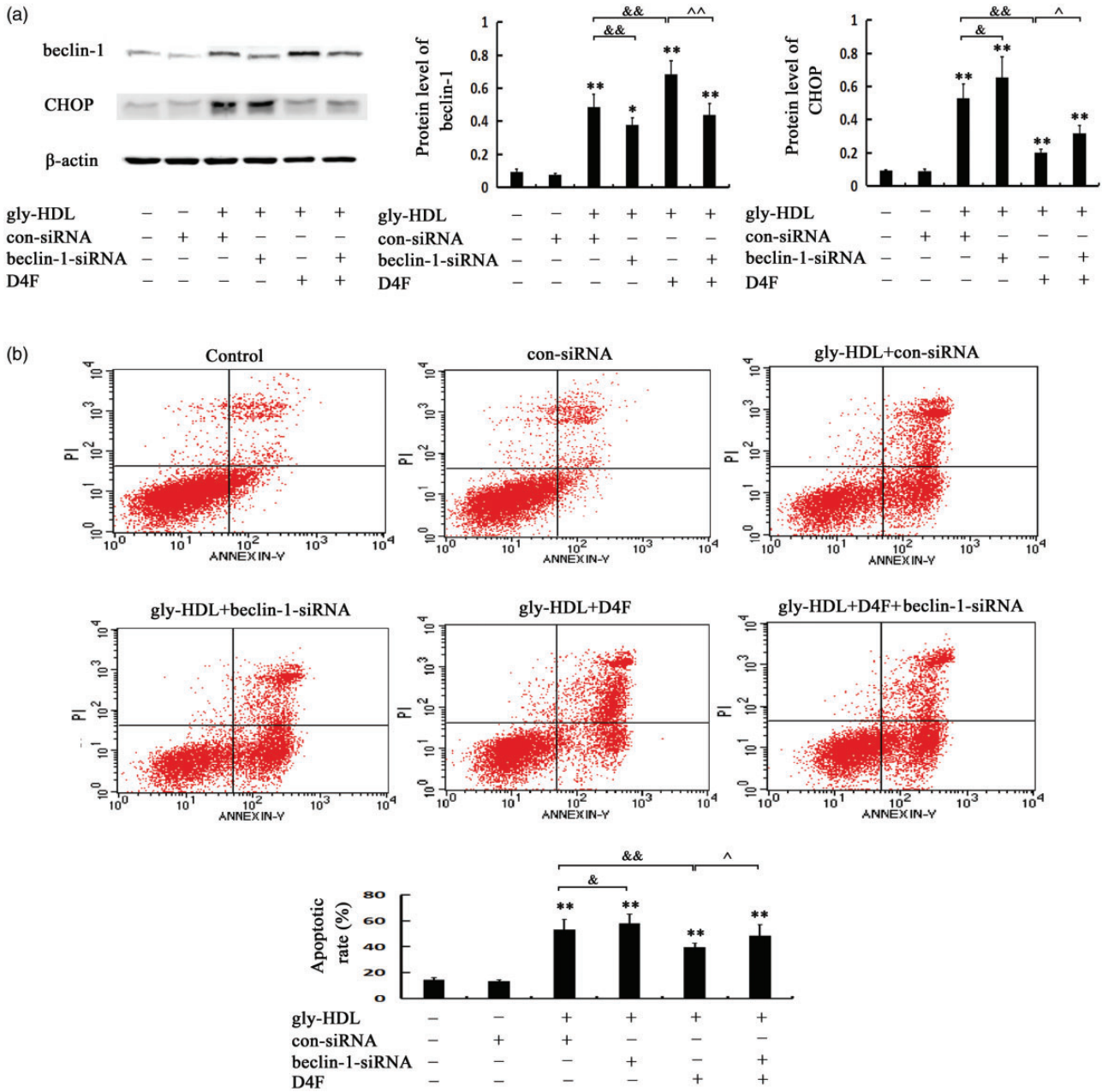


**Figure 7.** D4F inhibits CHOP-mediated apoptosis of RAW264.7 cells treated with gly-HDL by upregulating beclin-1. RAW264.7 cells were transfected with beclin-1 siRNA, followed by 100 mg/L gly-HDL treatment with or without D4F (50 mg/L) for 24 h. (a) Western blotting assay for assessing CHOP and beclin-1 levels. *n* = 4. (b) Cell apoptosis determined through flow cytometric analysis. *n* = 5. Mean ±SD. \**P* < 0.05, \*\**P* < 0.01 vs. Control group; &*P* < 0.05, &&*P* < 0.01. ^*P* < 0.05, ^^*P* < 0.01. (A color version of this figure is available in the online journal.)

progenitor cell proliferation, migration, and adhesion.<sup>17,35</sup> As revealed by our prior results, D4F alleviates the apoptosis of macrophages and human umbilical vein endothelial cells, mediated by ox-LDL, by inhibiting ER stress-CHOP signaling and downregulating the pigment epithelium-derived factor expression, respectively, indicating that D4F may work synergistically in both macrophages and endothelial cells at atherogenic sites.<sup>20,31</sup> However, few studies have reported the effects of D4F on gly-HDL-induced macrophage apoptosis and the underlying molecular mechanisms.

ER stress is well recognized as an adaptive response. Nonetheless, serious and persistent ER stress resulting

from pro-atherogenic factors, such as high levels of cholesterol and oxidative stress in advanced lesions, activates proapoptotic signals. As a key signal transduction molecule involved in ER stress-associated apoptosis, CHOP is significantly upregulated, mediates macrophage apoptosis, and subsequently leads to plaque necrosis and destabilization.<sup>11,36,37</sup> However, CHOP deficiency is proven to attenuate plaque necrosis and macrophage apoptosis in advanced AS plaque.<sup>11,36,38</sup> According to our prior results, ox-LDL and gly-HDL cause macrophage apoptosis by promoting CHOP upregulation.<sup>10,31</sup> The present study revealed that D4F remarkably inhibited the gly-HDL-induced macrophage injury and lipid accumulation which was

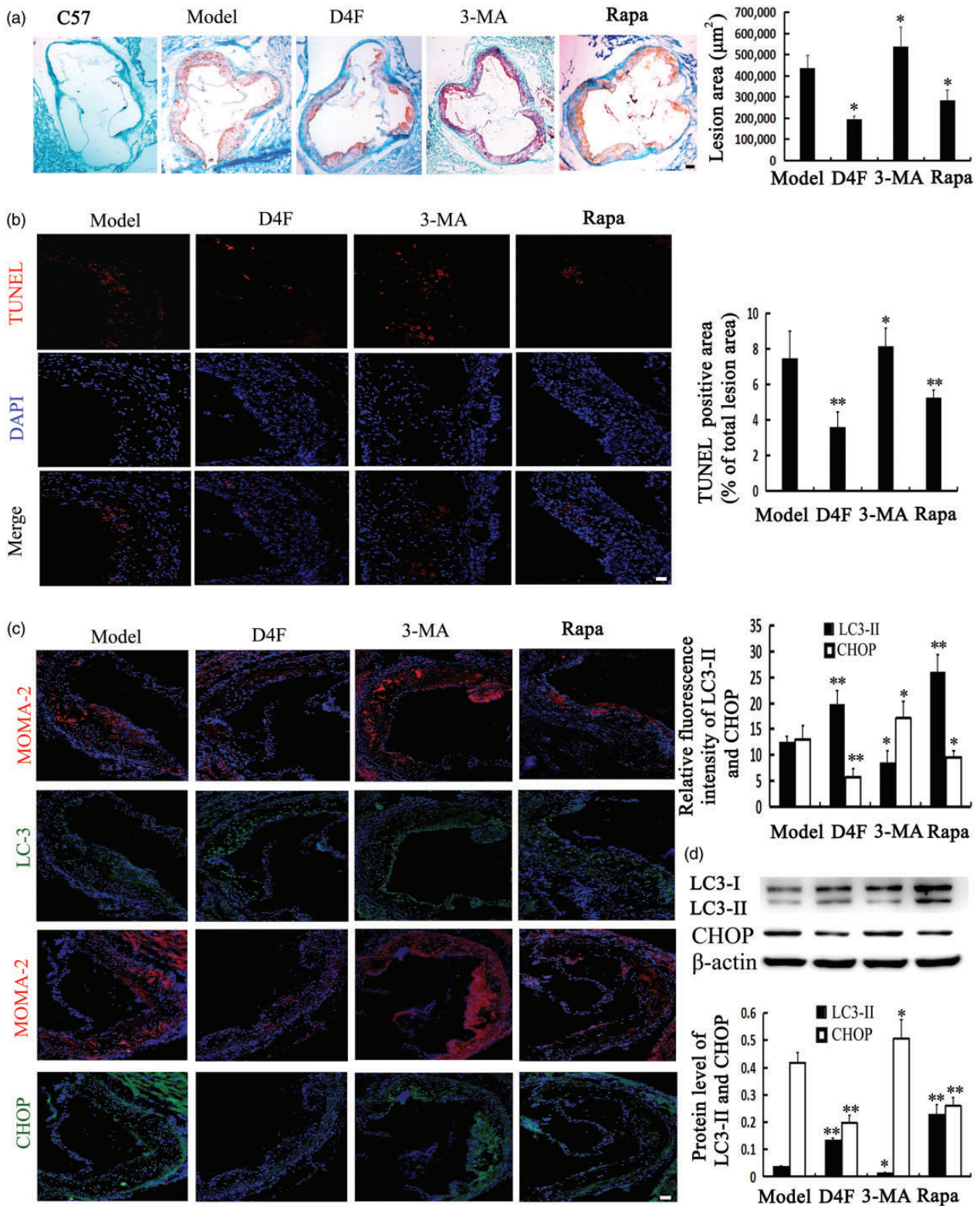


**Figure 8.** Role of D4F, 3-MA, and Rapa in atherosclerotic lesions and the expressions of LC3 and CHOP in diabetic apoE<sup>-/-</sup> mice. T2DM AS apoE<sup>-/-</sup> mice models were established and then intraperitoneally injected with vehicle (Model group), 1 mg/kg D4F (D4F group), 6 mg/kg rapamycin (Rapa group), or 50 mg/kg 3-methyladenine (3-MA group), daily for a total of 8 weeks. In addition, a normal chow diet was fed to male C57BL/6 mice as control. (a) Oil red O and brilliant green-stained aortic root cross-sections to examine the atherosclerosis lesion formation. Scale bar: 100  $\mu\text{m}$ ;  $n = 8$ . (b) Representative fluorescence micrographs depicting the TUNEL staining images for cell apoptosis (red) in the atherosclerosis lesions. Scale bar: 20  $\mu\text{m}$ ;  $n = 8$ . (c) Immunofluorescence staining in the presence of anti-MOMA-2, anti-CHOP, and anti-LC3-II antibodies. Scale bar: 20  $\mu\text{m}$ ;  $n = 6$ . Relative fluorescence intensities of LC3-II and CHOP (green) expression levels within the lesions rich in macrophages (red) were determined. (d) Western blotting assay to assess CHOP and LC3-II expressions within the aortic arches;  $n = 4$ . Mean  $\pm$  SD. \* $P < 0.05$ , \*\* $P < 0.01$  vs. model group. (A color version of this figure is available in the online journal.)

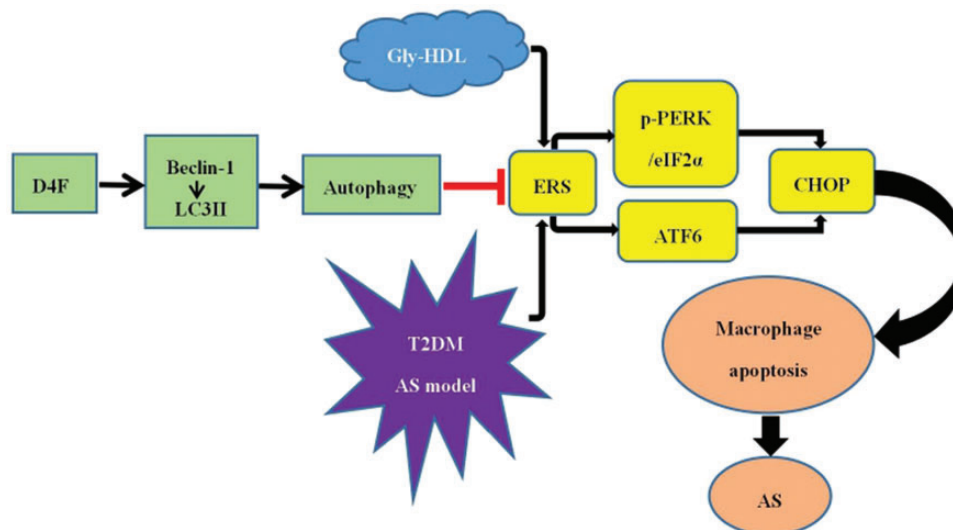


**Figure 9.** Schematic diagram of the molecular mechanism by which D4F alleviates C/EBP homologous protein-mediated apoptosis in glycated HDL-treated macrophages and T2DM AS. (A color version of this figure is available in the online journal.)

determined based on the reduced cell apoptosis and LDH leakage, enhanced cell viability, and inhibition of CHOP upregulation, consistent with PBA exposure. ATF6 and PERK are two key upstream molecules responsible for inducing CHOP upregulation,<sup>11,37</sup> which have also been proven to be involved in ox-LDL- and gly-HDL-mediated macrophage apoptosis in our previous works.<sup>10,31</sup> In the present work, it was demonstrated that similar to PBA, D4F also remarkably inhibited the upstream signals, evidenced by the decreased ATF6 nuclear translocation along with PERK and eIF2 $\alpha$  phosphorylation. According to these findings, D4F alleviates the gly-HDL-induced apoptosis of macrophages by suppressing the ER stress-CHOP axis.

Autophagy is a cytoprotective and recycling process involving the degradation of misfolded proteins or damaged organelles under pathological conditions.<sup>39</sup> Autophagy has been proven to protect against advanced atherosclerosis.<sup>26,27</sup> Autophagy induced by AGE-modified bovine serum albumin (AGE-BSA) protects against the AGE-BSA-caused damage to human vascular endothelial cells,<sup>33</sup> while the 7-ketocholesterol-activated autophagy alleviates the apoptosis of VSMCs by attenuating ER stress.<sup>32</sup> Consistently, the inhibition of autophagy results in endothelial dysfunction in patients with diabetes<sup>40</sup> and aggravates AS and VSMC apoptosis.<sup>41</sup> Our recent data revealed that rapamycin-stimulated autophagy diminished the gly-HDL-induced macrophage apoptosis and the ER stress-CHOP pathway.<sup>10</sup> The results of the present work revealed that D4F enhanced gly-HDL-triggered autophagy, as evidenced by the increased expressions of beclin-1, LC3-II, and ATG5 together with autophagosome accumulation in the macrophages. The promotion of autophagy by D4F abolished the upregulation of PERK phosphorylation, ATF6 nuclear translocation, and CHOP protein expression, and consequently, gly-HDL-induced macrophage apoptosis. In addition, the protective effects of D4F were further enhanced by rapamycin and alleviated by 3-MA and

beclin-1 siRNA treatments. Moreover, the attenuation of autophagy by 3-MA aggravated cell apoptosis, atherosclerotic lesions, and CHOP upregulation in T2DM apoE<sup>-/-</sup> mice. Consistently, similar to rapamycin, D4F increased the LC3-II level while reducing CHOP level, cell apoptosis, and atherosclerotic lesions.

In summary, our findings indicated that D4F could attenuate apoptosis of gly-HDL-treated macrophages induced by ER stress-CHOP by facilitating autophagy. As verified in a clinical test, oral administration of D4F presented high safety and could enhance the anti-inflammatory effects of HDL.<sup>42</sup> Therefore, mimetic peptides are becoming increasingly recognized as the possible efficient tool to treat AS and the associated cardiovascular disorders. The findings of the present work also suggest that D4F has different physiological effects. Therefore, the present study supports the application of D4F in the pharmacological treatment of AS in T2DM and provides a foundation for the clinical application of D4F.

#### AUTHORS' CONTRIBUTIONS

HT was responsible for collecting and analyzing data and drafting manuscripts. ZZ and XH performed cell culture, TUNEL, and immunofluorescence assay. TP performed CCK8 assay, oil red O staining, Western blotting analysis, and animal experiments. LZ helped to carry out animal experiments. XW made a contribution to preparing gly-HDL. PJ was responsible for flow cytometric analysis. LY, GT, and YY conducted cell studies. SQ assisted in study design. HT and SY contributed to study design and funding. All the authors approved the eventual manuscript for publication.

#### DECLARATION OF CONFLICTING INTERESTS

The author(s) declared no potential conflicts of interest with respect to the research, authorship, and/or publication of this article.

## FUNDING

The present study was supported by the National Natural Science Foundations of China (81800394, 81570410) and the Academic promotion program of Shandong First Medical University (2019QL010).

## ORCID iD

Hua Tian  <https://orcid.org/0000-0001-5606-9582>

## REFERENCES

- Haffner1 SM, Lehto S, Rönnemaa T, Pyörälä K, Laakso M. Mortality from coronary heart disease in subjects with type 2 diabetes and in nondiabetic subjects with and without prior myocardial infarction. *N Engl J Med* 1998;**339**:229–34
- Engelgau MM, Geiss LS, Saaddine JB. The evolving diabetes burden in the United States. *Ann Intern Med* 2004;**140**:945–50
- Kumar P, Swain MM, Pal A. Hyperglycemia-induced inflammation caused down-regulation of 8-oxoG-DNA glycosylase levels in murine macrophages is mediated by oxidative-nitrosative stress-dependent pathways. *Int J Biochem Cell Biol* 2016;**73**:82–98
- Rani K, Aung NY. Docosahexaenoic acid inhibits vascular smooth muscle cell proliferation induced by glucose variability. *Open Biochem J* 2017;**11**:56–65
- Byun K, Yoo Y, Son M, Lee J, Jeong GB, Park YM, Salekdeh GH, Lee B. Advanced glycation end-products produced systemically and by macrophages: a common contributor to inflammation and degenerative diseases. *Pharmacol Ther* 2017;**177**:44–55
- Xu L, Wang YR, Li PC, Feng B. Advanced glycation end products increase lipids accumulation in macrophages through upregulation of receptor of advanced glycation end products: increasing uptake, esterification and decreasing efflux of cholesterol. *Lipids Health Dis* 2016;**15**:161
- Liu D, Ji L, Zhao M, Wang Y, Guo Y, Li L, Zhang D, Xu L, Pan B, Su J, Xiang S, Pennathur S, Li J, Gao J, Liu P, Willard B, Zheng L. Lysine glycation of apolipoprotein A-I impairs its anti-inflammatory function in type 2 diabetes mellitus. *J Mol Cell Cardiol* 2018;**122**:47–57
- Brinck JW, Thomas A, Lauer E, Jornayvaz FR, Brulhart-Meynet MC, Prost JC, Pataky Z, Lofgren P, Hoffstedt J, Eriksson M, Pramfalk C, Morel S, Kwak BR, van Eck M, James RW, Frias MA. Diabetes mellitus is associated with reduced high-density lipoprotein sphingosine-1-phosphate content and impaired high-density lipoprotein cardiac cell protection. *Arterioscler Thromb Vasc Biol* 2016;**36**:817–24
- Matsunaga T, Iguchi K, Nakajima T, Koyama I, Miyazaki T, Inoue I, Kawai S, Katayama S, Hirano K, Hokari S, Komoda T. Glycated high-density lipoprotein induces apoptosis of endothelial cells via a mitochondrial dysfunction. *Biochem Biophys Res Commun* 2001;**287**:714–20
- Tian H, Li Y, Kang P, Wang Z, Yue F, Jiao P, Yang N, Qin S, Yao S. Endoplasmic reticulum stress-dependent autophagy inhibits glycated high-density lipoprotein-induced macrophage apoptosis by inhibiting CHOP pathway. *J Cell Mol Med* 2019;**23**:2954–69
- Tsukano H, Gotoh T, Endo M, Miyata K, Tazume H, Kadomatsu T, Yano M, Iwawaki T, Kohno K, Araki K, Mizuta H, Oike Y. The endoplasmic reticulum stress-C/EBP homologous protein pathway-mediated apoptosis in macrophages contributes to the instability of atherosclerotic plaques. *Arterioscler Thromb Vasc Biol* 2010;**30**:1925–32
- Dickhout JG, Colgan SM, Lhotak S, Austin RC. Increased endoplasmic reticulum stress in atherosclerotic plaques associated with acute coronary syndrome: a balancing act between plaque stability and rupture. *Circulation* 2007;**116**:1214–6
- Yao S, Tian H, Zhao L, Li J, Yang L, Yue F. Oxidized high density lipoprotein induces macrophage apoptosis via toll-like receptor 4-dependent CHOP pathway. *J Lipid Res* 2017;**58**:164–77
- Navab M, Anantharamaiah GM, Reddy ST, Hama S, Hough G, Grijalva VR, Yu N, Ansell BJ, Datta G, Garber DW, Fogelman AM. Apolipoprotein A-I mimetic peptides. *Arterioscler Thromb Vasc Biol* 2005;**25**:1325–31
- Navab M, Anantharamaiah GM, Reddy ST. Peptide mimetics of apolipoproteins improve HDL function. *J Clin Lipidol* 2007;**1**:142–7
- Navab M, Anantharamaiah GM, Reddy ST, Hama S, Hough G, Grijalva VR, Wagner AC, Frank JS, Datta G, Garber D, Fogelman AM. Oral D-4F causes formation of pre-beta high-density lipoprotein and improves high-density lipoprotein-mediated cholesterol efflux and reverse cholesterol transport from macrophages in apolipoprotein E-null mice. *Circulation* 2004;**109**:3215–20
- Xie Q, Zhao SP, Li F. D-4F, an apolipoprotein A-I mimetic peptide, promotes cholesterol efflux from macrophages via ATP-binding cassette transporter A1. *Tohoku J Exp Med* 2010;**220**:223–8
- Morgantini C, Imaizumi S, Grijalva V, Navab M, Fogelman AM, Reddy ST. Apolipoprotein A-I mimetic peptides prevent atherosclerosis development and reduce plaque inflammation in a murine model of diabetes. *Diabetes* 2010;**59**:3223–8
- Navab M, Anantharamaiah GM, Hama S, Garber DW, Chaddha M. Oral administration of an Apo A-I mimetic peptide synthesized from D-amino acids dramatically reduces atherosclerosis in mice independent of plasma cholesterol. *Circulation* 2002;**105**:290–2
- Liu Y, Yao S, Wang S, Jiao P, Song G, Yu Y, Zhu P, Qin S. D-4F, an apolipoprotein A-I mimetic peptide, protects human umbilical vein endothelial cells from oxidized low-density lipoprotein-induced injury by preventing the downregulation of pigment epithelium-derived factor expression. *J Cardiovasc Pharmacol* 2014;**63**:553–61
- Tian H, Yao ST, Yang NN, Ren J, Jiao P, Zhang X, Li DX, Zhang GA, Xia ZF, Qin SC. D4F alleviates macrophage-derived foam cell apoptosis by inhibiting the NF-kappaB-dependent Fas/FasL pathway. *Sci Rep* 2017;**7**:7333
- Zhang C, Syed TW, Liu R, Yu J. Role of endoplasmic reticulum stress, autophagy, and inflammation in cardiovascular disease. *Front Cardiovasc Med* 2017;**4**:
- Vurusaner B, Gargiulo S, Testa G, Gamba P, Leonarduzzi G, Poli G, Basaga H. The role of autophagy in survival response induced by 27-hydroxycholesterol in human promonocytic cells. *Redox Biol* 2018;**17**:400–10
- Park HS, Han JH, Jung SH, Lee DH, Heo KS, Myung CS. Anti-apoptotic effects of autophagy via ROS regulation in microtubule-targeted and PDGF-stimulated vascular smooth muscle cells. *Korean J Physiol Pharmacol* 2018;**22**:349–60
- Zou X, Xu J, Yao S, Li J, Yang Y, Yang L. Endoplasmic reticulum stress-mediated autophagy protects against lipopolysaccharide-induced apoptosis in HL-1 cardiomyocytes. *Exp Physiol* 2014;**99**:1348–58
- Liao X, Sluimer JC, Wang Y, Subramanian M, Brown K, Pattison JS, Robbins J, Martinez J, Tabas I. Macrophage autophagy plays a protective role in advanced atherosclerosis. *Cell Metab* 2012;**15**:545–53
- Peng S, Xu LW, Che XY, Xiao QQ, Pu J, Shao Q, He B. Atorvastatin inhibits inflammatory response, attenuates lipid deposition, and improves the stability of vulnerable atherosclerotic plaques by modulating autophagy. *Front Pharmacol* 2018;**9**:
- Hedrick CC, Thorpe SR, Fu MX, Harper CM, Yoo J, Kim SM, Wong H, Peters AL. Glycation impairs high-density lipoprotein function. *Diabetologia* 2000;**43**:312–20
- Ren S, Shen GX. Impact of antioxidants and HDL on glycated LDL-induced generation of fibrinolytic regulators from vascular endothelial cells. *Arterioscler Thromb Vasc Biol* 2000;**20**:1688–93
- Liu MH, Li Y, Han L, Zhang YY, Wang D, Wang ZH, Zhou HM, Song M, Li YH, Tang MX, Zhang W, Zhong M. Adipose-derived stem cells were impaired in restricting CD4<sup>+</sup> T cell proliferation and polarization in type 2 diabetic ApoE<sup>-/-</sup> mouse. *Mol Immunol* 2017;**87**:152–60
- Yao S, Tian H, Miao C, Zhang DW, Zhao L, Li Y, Yang N, Jiao P, Sang H, Guo S, Wang Y, Qin S. D4F alleviates macrophage-derived foam cell apoptosis by inhibiting CD36 expression and ER stress-CHOP pathway. *J Lipid Res* 2015;**56**:836–47
- He C, Zhu H, Zhang W, Okon I, Wang Q, Li H, Le YZ, Xie Z. 7-Ketocholesterol induces autophagy in vascular smooth muscle cells through Nox4 and Atg4B. *Am J Pathol* 2013;**183**:626–37

33. Xie Y, You SJ, Zhang YL, Han Q, Cao YJ, Xu XS, Yang YP, Li J, Liu CF. Protective role of autophagy in AGE-induced early injury of human vascular endothelial cells. *Mol Med Rep* 2011;**4**:459–64
34. Stoekenbroek RM, Stroes ES, Hovingh GK. ApoA-I mimetics. *Handb Exp Pharmacol* 2015;**224**:631–48
35. Zhang Z, Qun J, Cao C, Wang J, Li W, Wu Y, Du L, Zhao P, Gong K. Apolipoprotein A-I mimetic peptide D-4F promotes human endothelial progenitor cell proliferation, migration, adhesion through eNOS/NO pathway. *Mol Biol Rep* 2012;**39**:4445–54
36. Yu X, Wang Y, Zhao W, Zhou H, Yang W, Guan X. Toll-like receptor 7 promotes the apoptosis of THP-1-derived macrophages through the CHOP-dependent pathway. *Int J Mol Med* 2014;**34**:886–93
37. Myoishi M, Hao H, Minamino T, Watanabe K, Nishihira K, Hatakeyama K, Asada Y, Okada K, Ishibashi-Ueda H, Gabbiani G, Bochaton-Piallat ML, Mochizuki N, Kitakaze M. Increased endoplasmic reticulum stress in atherosclerotic plaques associated with acute coronary syndrome. *Circulation* 2007;**116**:1226–33
38. Thorp E, Li G, Seimon TA, Kuriakose G, Ron D, Tabas I. Reduced apoptosis and plaque necrosis in advanced atherosclerotic lesions of Apoe<sup>-/-</sup> and Ldlr<sup>-/-</sup> mice lacking CHOP. *Cell Metab* 2009;**9**:474–81
39. Ravanan P, Srikumar IF, Talwar P. Autophagy: the spotlight for cellular stress responses. *Life Sci* 2017;**188**:53–67
40. Zhang H, Ge S, He K, Zhao X, Wu Y, Shao Y, Wu X. FoxO1 inhibits autophagosome-lysosome fusion leading to endothelial autophagic-apoptosis in diabetes. *Cardiovasc Res* 2019;**115**:2008–20
41. Osonoi Y, Mita T, Azuma K, Nakajima K, Masuyama A, Goto H, Nishida Y, Miyatsuka T, Fujitani Y, Koike M, Mitsumata M, Watada H. Defective autophagy in vascular smooth muscle cells enhances cell death and atherosclerosis. *Autophagy* 2018;**14**:1991–2006
42. Bloedon LT, Dunbar R, Duffy D, Pinell-Salles P, Norris R, DeGroot BJ, Movva R, Navab M, Fogelman AM, Rader DJ. Safety, pharmacokinetics, and pharmacodynamics of oral apoA-I mimetic peptide D-4F in high-risk cardiovascular patients. *J Lipid Res* 2008;**49**:1344–52

(Received June 18, 2021, Accepted August 23, 2021)